A Scaffold-Assisted 3D Cancer Cell Model for Surface-Enhanced Raman Scattering-Based Real-Time Sensing and Imaging

Clara García-Astrain[1,2], Malou Henriksen-Lacey[1,2]*, Elisa Lenzi[1,#], Carlos Renero-Lecuna[1,3], Judith Langer[1], Paula Piñeiro[1,4], Beatriz Molina-Martínez[1,¥], Javier Plou[1,$], Dorleta Jimenez de Aberasturi[1,2,5], Luis M. Liz-Marzán[1,2,3,5]**

[1]CIC biomaGUNE, Basque Research and Technology Alliance (BRTA), 20014 Donostia-San Sebastián, Spain

[2]Centro de Investigación Biomédica en Red, Bioingeniería, Biomateriales y Nanomedicina (CIBER-BBN), 20014 Donostia-San Sebastián, Spain

[3]Cinbio, University of Vigo, 36310 Vigo, Spain

[4]Department of Applied Chemistry, University of the Basque Country (UPV-EHU), 20018 Donostia-San Sebastián, Spain

[5]Ikerbasque, Basque Foundation for Science, 48009 Bilbao, Spain

*E-mail: cgarcia@cicbiomagune.es, mhenriksen@cicbiomagune.es, llizmarzan@cicbiomagune.es

[#]Current address: Institut Pasteur, Université Paris Cité, 75015 Paris, France, France

[¥]Current address: Biobide Spain (BBD BIOPHENIX, S.L.U.), 20009 Donostia-San Sebastian, Spain.

[$]Current address: CIC nanoGUNE, Basque Research and Technology Alliance (BRTA), 20018 Donostia-San Sebastián, Spain

Summary of contents

1. Nanoparticle characterization

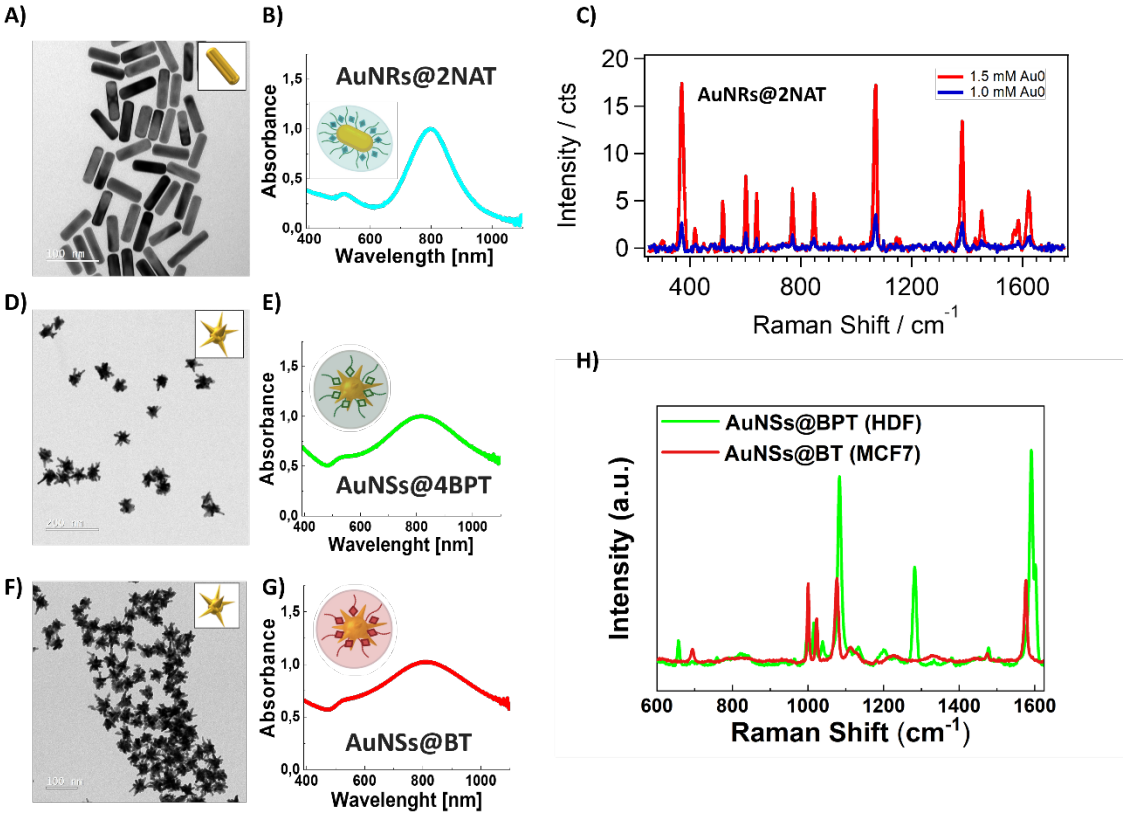

Figure S1. TEM images, UV-vis-NIR spectra and characteristic SERS spectra of the different nanoparticles used in this work. (**A-C**) For scaffold labeling, AuNRs coated with 2NAT were employed, SERS spectra of scaffolds labeled with AuNR@2NAT with varying AuNR concentration are shown. (**D-H**) For cell labeling, AuNSs coated with BT or BPT were employed. Characteristic SERS fingerprints of labeled AuNSs internalized by HDF and MCF7 cells are shown.

2. Scaffold Characterization

2.1.Rheology, swelling and biocompatibility

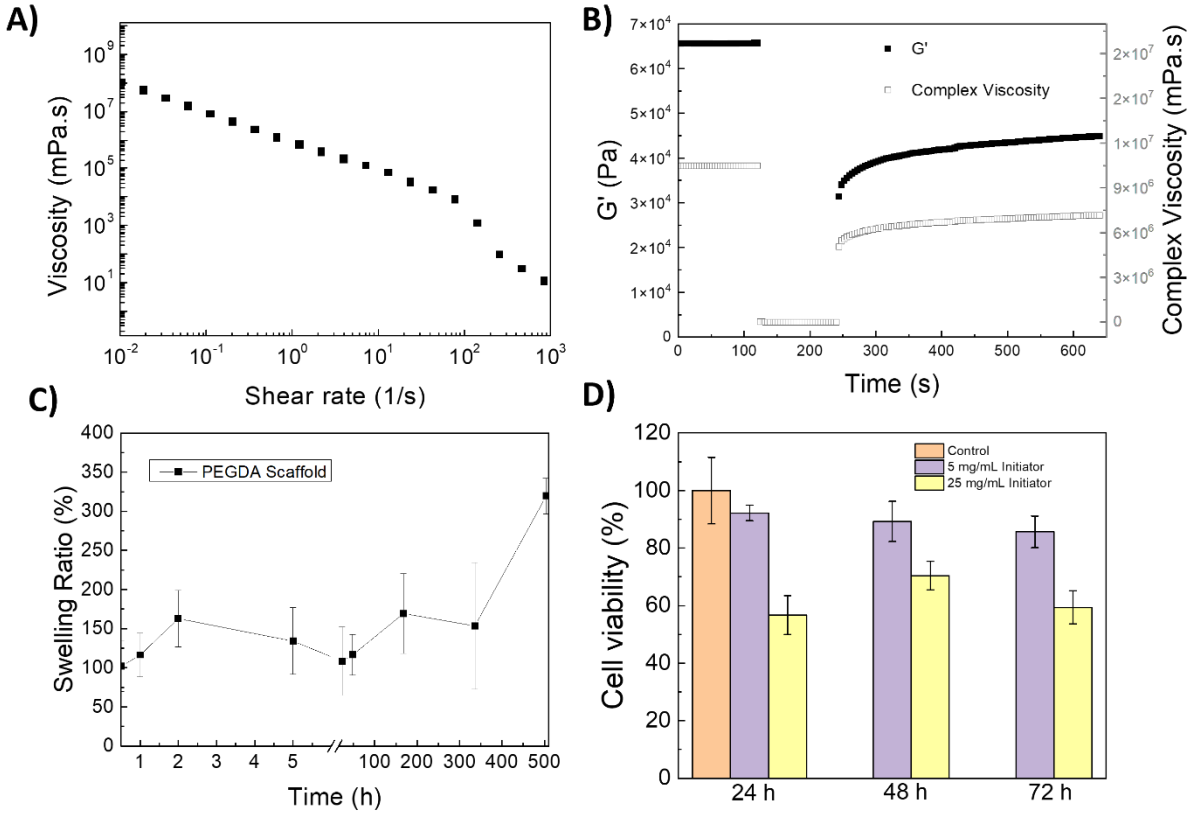

Figure S2. A) Flow curve of PEGDA-based ink. **B)** Thixotropy tests of PEGDA-based ink (G' (black dots) are plotted in the left axis and complex viscosity (open dots) are plotted in the right axis). **C)** Swelling ratio for the printed scaffold in cDMEM at 37 °C (n=3). **D)** MCF7 viability test, in contact with scaffolds prepared with different concentrations of the Irgacure 2959 photoinitiator.

2.2. Scaffold stability

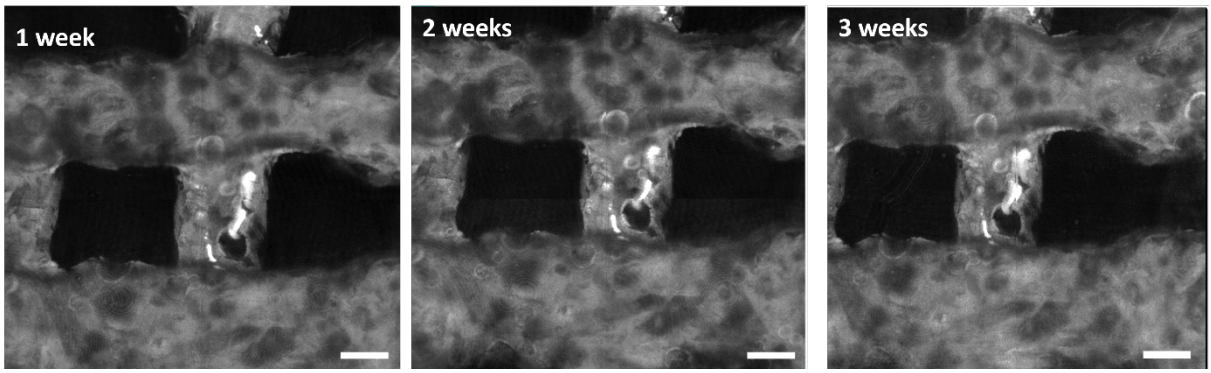

Figure S3. Maximum intensity projection (MIP) images of a Z-stack showing the scaffold incubated in PBS for up to 3 weeks. The scaffold was imaged using reflection microscopy (scale bar = 200 µm).

2.3.SERS mapping

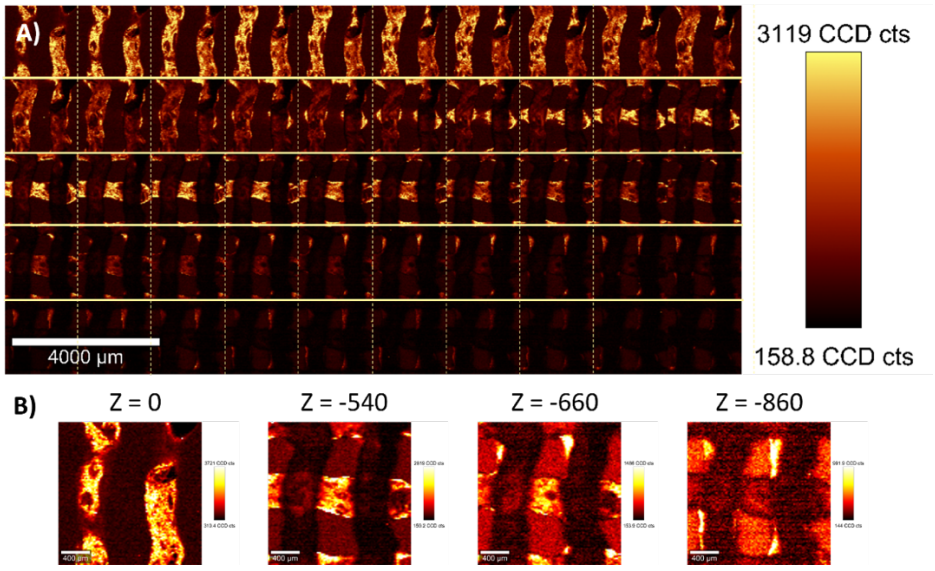

Figure S4. SERS maps of the intensity of the MBA peak at 1084 cm^{-1}, showing XY planes at different heights of the scaffold. **A)** All the different planes scanned every 30 µm; **B)** Four specific planes at specific Z heights, as labelled.

3. Coated scaffolds for cell growth

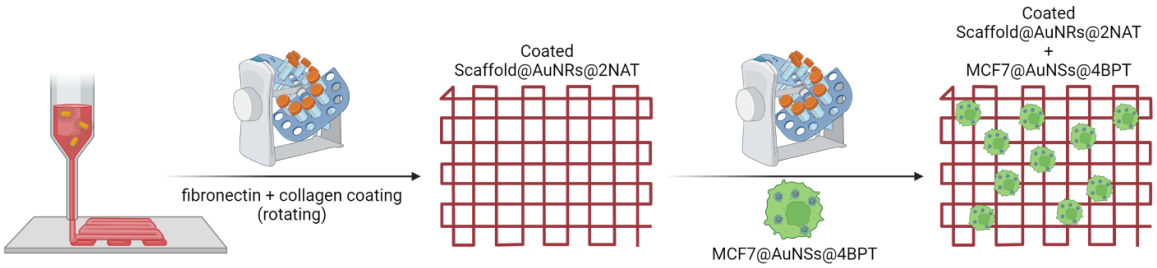

Figure S5. Schematic representation of the preparation of ECM-coated labelled scaffolds for 3D cell model growth.

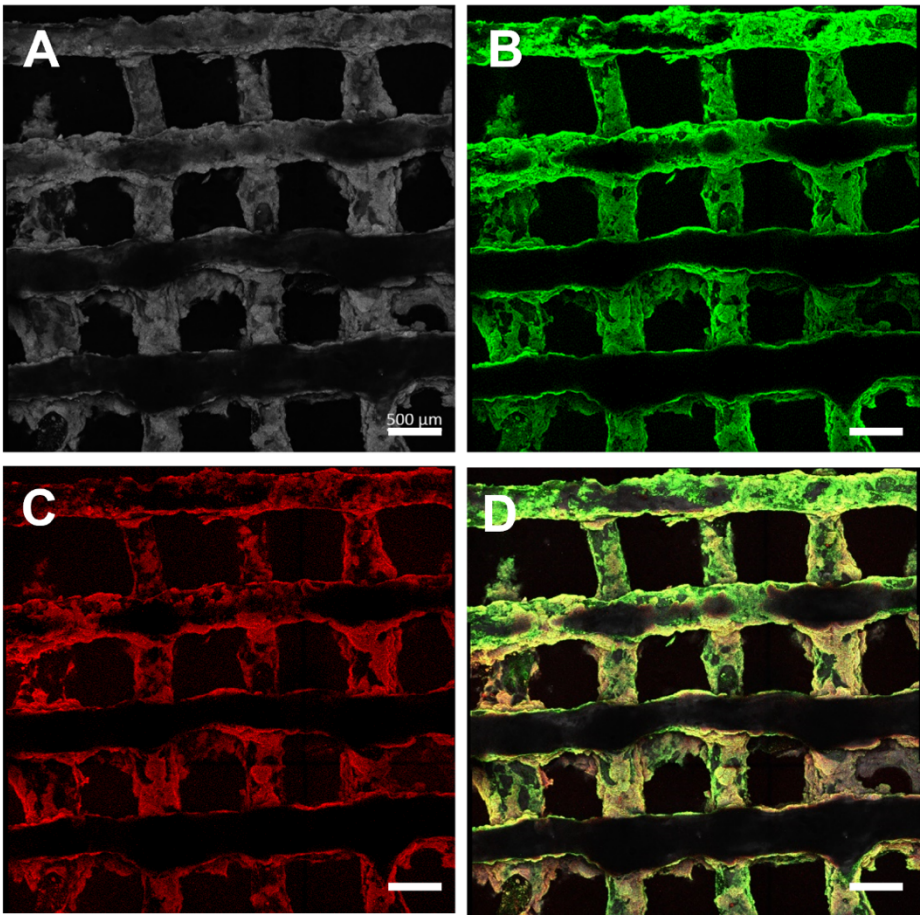

Figure S6. Immunofluorescence staining of scaffolds to show the presence of fibronectin and collagen. MIP images of a Z-stack (1532 x 1532 x 374 µm, XYZ) show the scaffold, imaged using: reflection microscopy (**A**, grey scale), fibronectin (**B**, green), collagen (**C**, red), and a merged image (**D**). Scale bars: 500 µm.

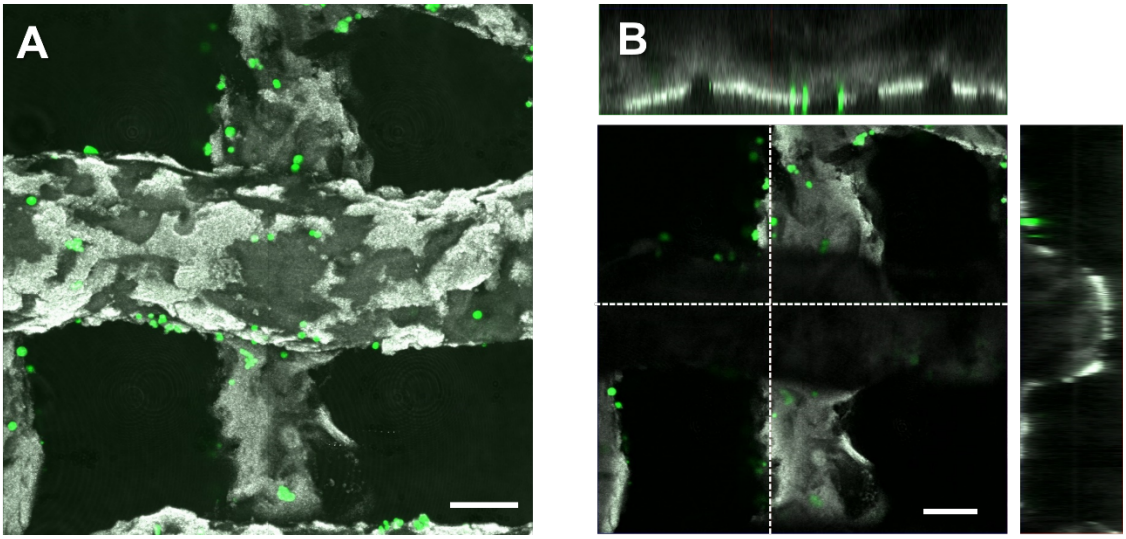

Figure S7. Cell adhesion to ECM-coated scaffolds. **A)** MIP image of a Z-stack (1532 × 1532 × 374 µm, XYZ) showing the scaffold (reflection microscopy, in greyscale), and MCF7 cells (GFP expressing, in green). **B)** Orthogonal image showing XZ and YZ profiles from the coordinates marked with dotted lines in the central XY image. Scale bars: 200 µm.

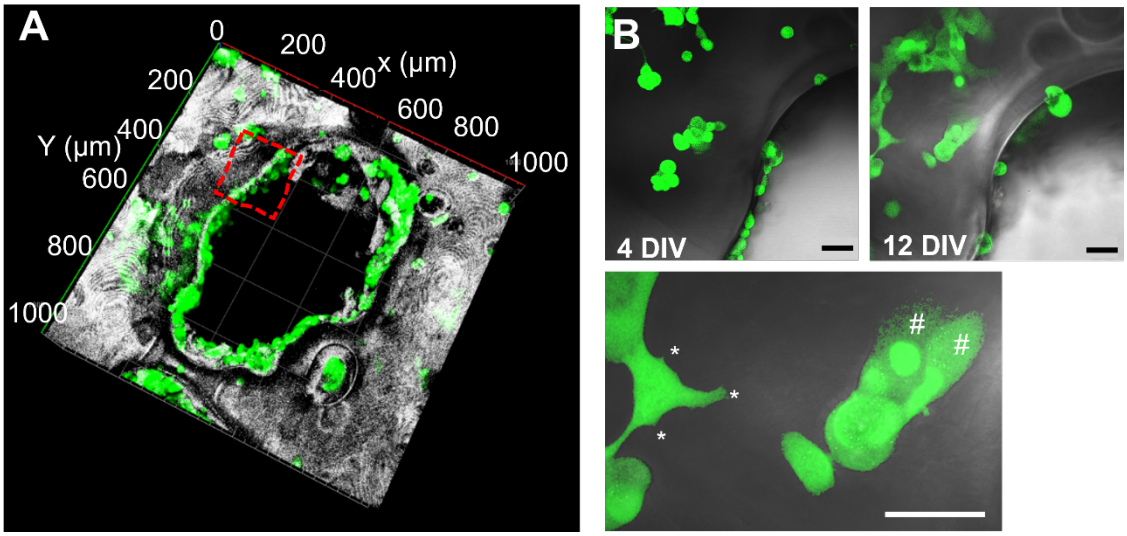

Figure S8. Cell adhesion to ECM-coated scaffolds. **A)** 3D rendition of Z-stack (1000 µm × 1000 µm × 250 µm, XYZ) showing the distribution of MCF7 cells (GFP expressing, in green) around an imaging window. **B)** Higher magnification images of the red-dashed area in (A), showing changes in cell morphology with time, characterized by the formation of lamellipodia (#) and filopodia (*) (lower image). Scale bars: 50 µm.

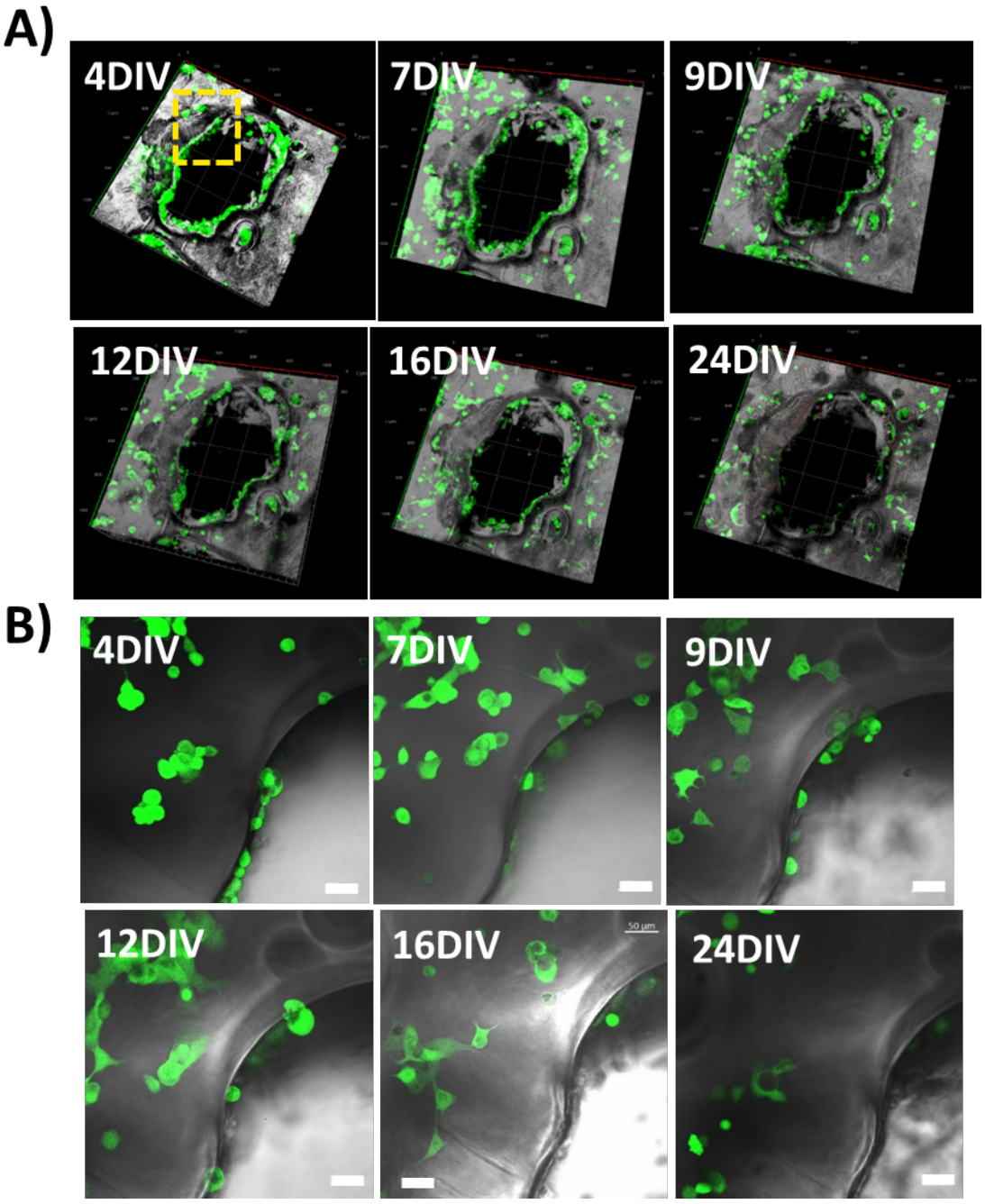

Figure S9. Cell adhesion to ECM-coated scaffolds. **A)** 3D renditions of Z-stacks (ca. 1000 µm × 1000 µm × 250 µm, XYZ) showing the scaffold structure in greyscale (imaged using reflection microscopy), and the cells in green (GFP expressing). **B)** MIP images of Z-stacks from the scaffold area indicated by the yellow dotted square in A (4DIV). Scale bars: 50 µm.

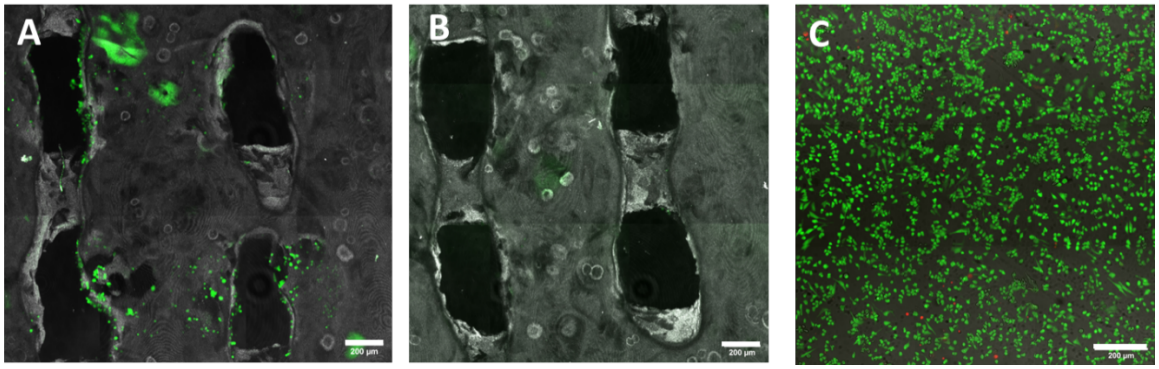

Figure S10. Effect of ECM components promoting successful adherence of MCF7 cells (GFP expressing, in green) onto the surface of the scaffold. Scaffolds are shown with (**A**) and without (**B**) fibronectin and collagen surface coatings. **C)** Underlying substrate of a scaffold without ECM functionalization, showing cells that passed through the scaffold. Scale bars: 200 µm.

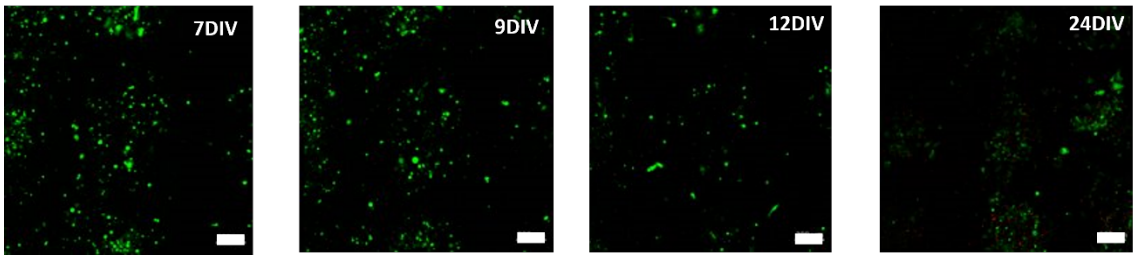

Figure S11. Presence of MCF7 cells (GFP expressing, in green) on the underlying substrate supporting the scaffold. Whereas at early timepoints (7 DIV) numerous cells were observed, no increase in cell number was observed over time. Scale bars: 200 µm.

4. 3D cell growth within scaffold + Matrigel model

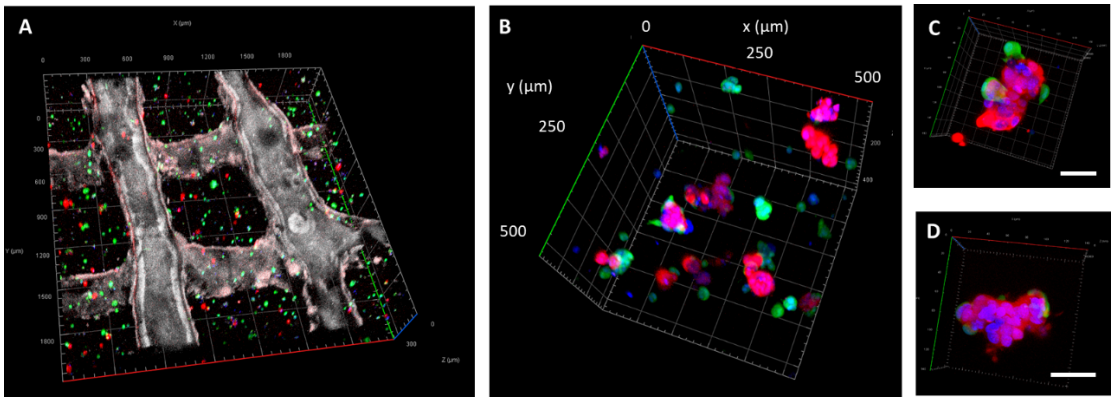

Figure S12. **A)** 3D reconstruction of the live cell imaging of MCF7 (RFP expressing, red) and HDF (GFP expressing, in green) cells, suspended in Matrigel (3.7 mg/mL) inside a PEGDA scaffold (reflection imaging, in white). **B-D)** In situ spheroid formation, showing HDF cells growing around MCF7 cell aggregates (NucBlue staining shows cell nuclei). Scale bars: 50 µm. Images were obtained after 5 DIV.

5. SERS Imaging within scaffold + Matrigel model

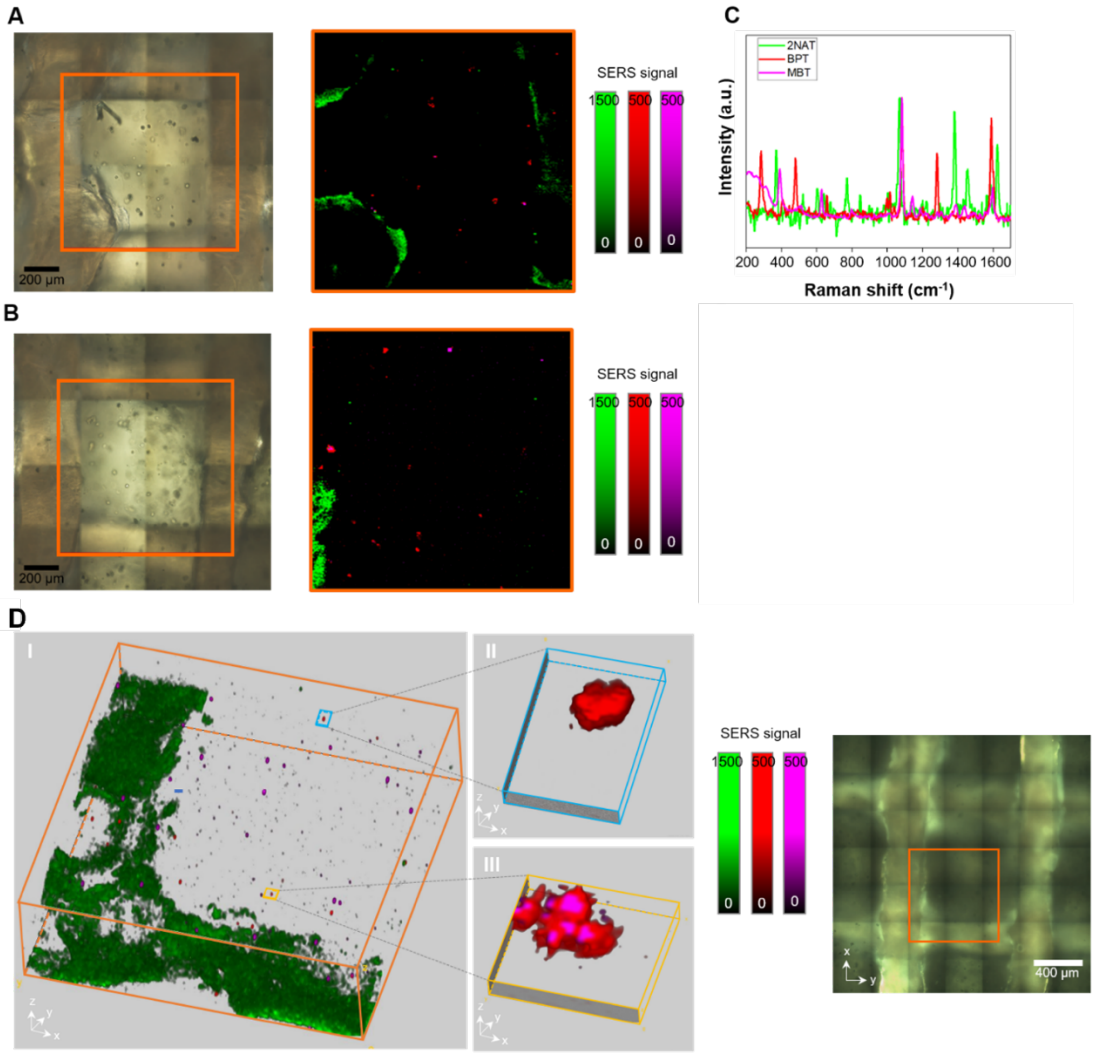

Figure S13. SERS images of a PEGDA scaffold containing MCF7 and HDF cells grown in Matrigel. **A,B)** Optical images and correlated 2D SERS maps of 1000 µm × 1000 µm areas of the scaffold in the XY plane, with 5 µm step size in both directions. The signal of the hydrogel-based scaffold labelled with AuNS@2NAT, and both cell types, MCF7 labeled with AuNS@MBT and HDFs labelled with AuNS@4BPT, are reported respectively in green, red and magenta. **C)** Representative peaks for each SERS tag: 1070 cm^{-1}, 1383 cm^{-1}, 1626 cm^{-1} for 2NAT; 1084 cm^{-1}, 1593 cm^{-1}, 1604 cm^{-1} for 4BPT; 1082 cm^{-1}, 1597 cm^{-1} for MBT. **D)** 3D volume reconstruction of SERS maps (I) imaged under live conditions after 5 DIV (total area 750 µm × 750 µm × 500 µm, with step sizes of 5 µm × 5 µm × 20 µm in XYZ directions), with two highlighted volumetric regions, a single HDF cell (II) and an aggregate of MCF7 and HDF cells (III), and optical image of the scaffold.

6. 3D cell growth with preformed spheroids in scaffold + optimized ECM model

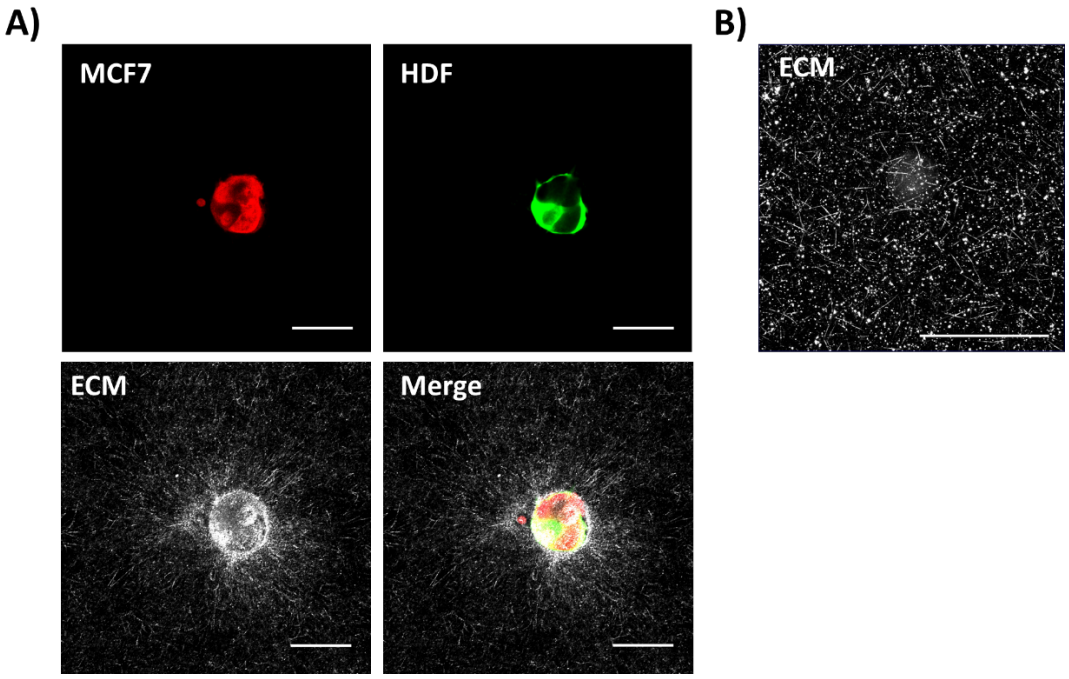

Figure S14. Spheroid-induced remodeling of the ECM. Optimized ECM was imaged with (**A**) and without (**B**) cells or spheroids. Using reflection microscopy with excitation at 488 nm and with the emission detector set at 485 – 493 nm, we observed changes in ECM organization around spheroids, resembling fibers radially branching from the spheroid surface.[1] Scale bars, 50 μm.

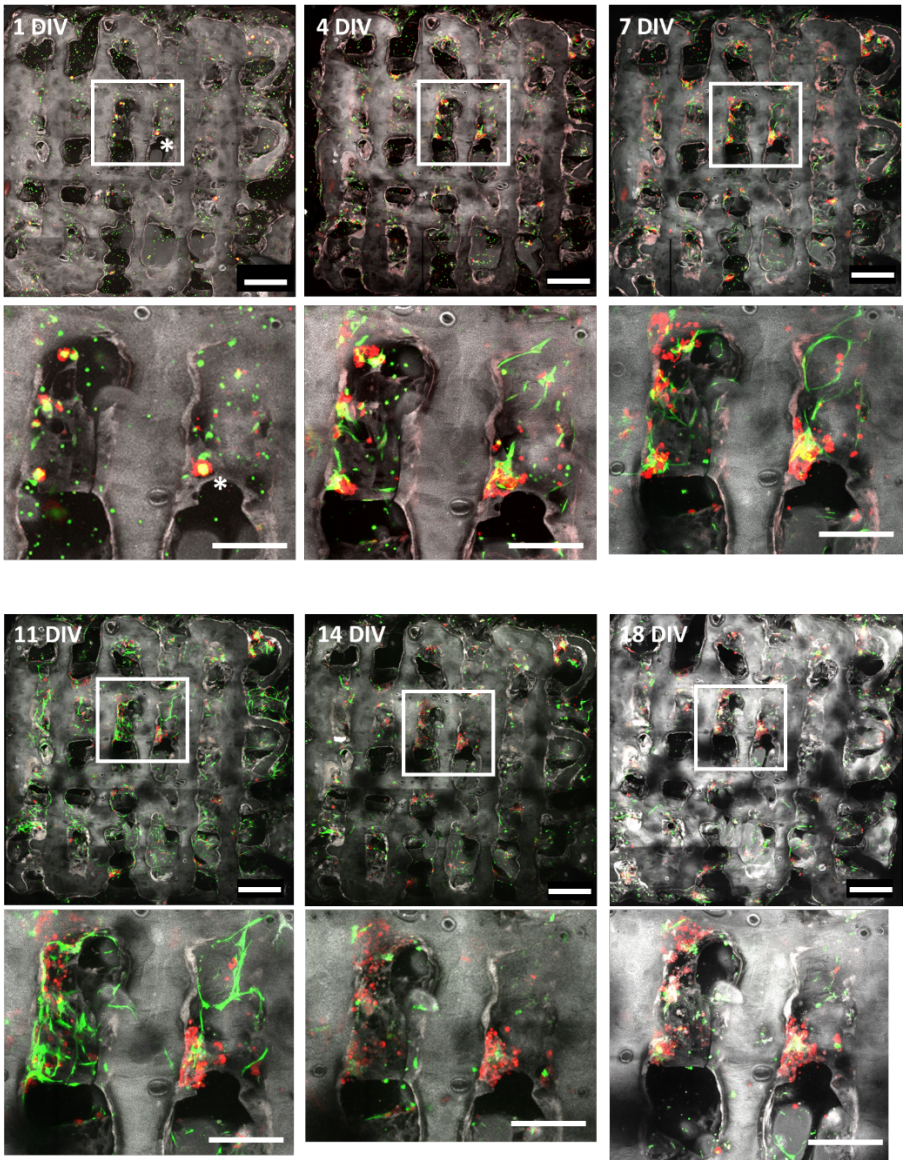

Figure S15. MIP images from confocal microscopy Z-stacks of scaffolds containing MCF7 (expressing RFP) and HDF (expressing GFP) cells growing in optimized ECM, surrounding a PEGDA scaffold (imaged using reflection microscopy). The whole scaffold and a zoom of the area indicated by the white square are shown, for timepoints up to 18 DIV, as labelled. The spheroid marked with a white * at 1 DIV is shown in more detail in Figure S17. Whole scaffold scale bars: 1mm; zoom image scale bars: 500 µm.

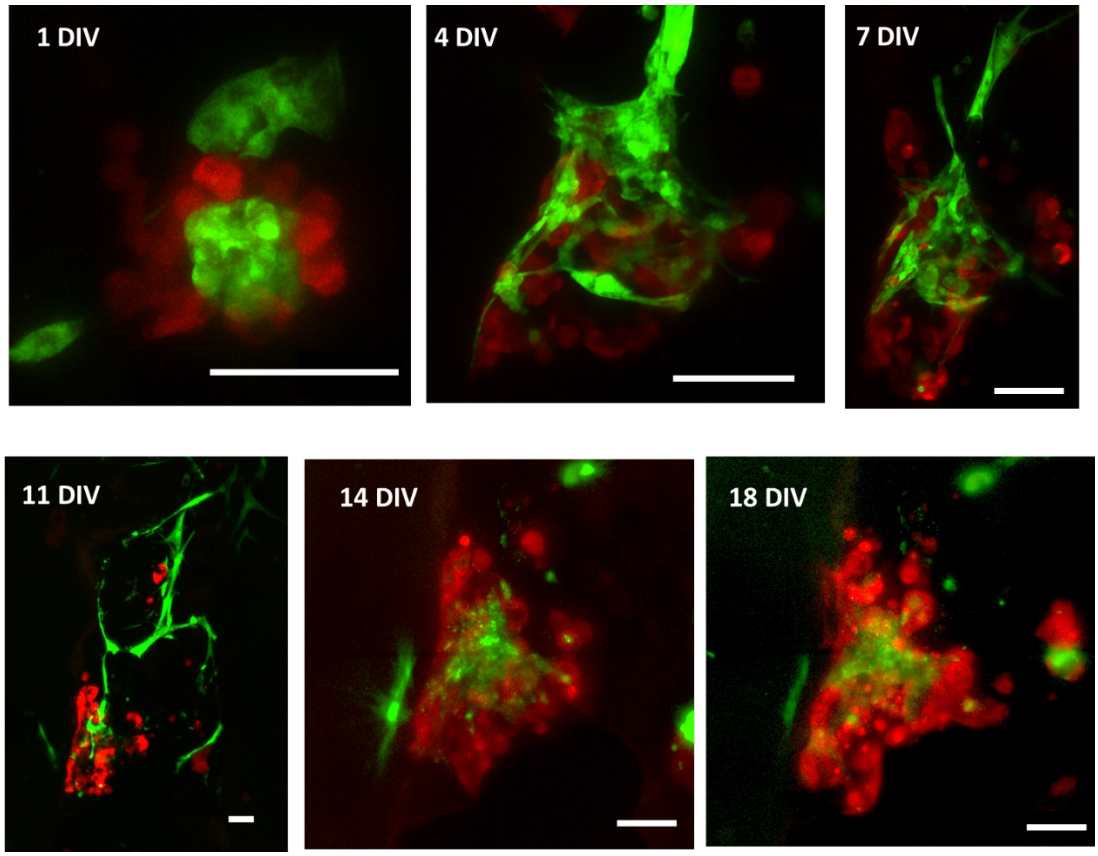

Figure S16. MIP fluorescence images showing the growth of a single spheroid (indicated by * in the first image set of Figure S15). Scale bars: 100 µm.

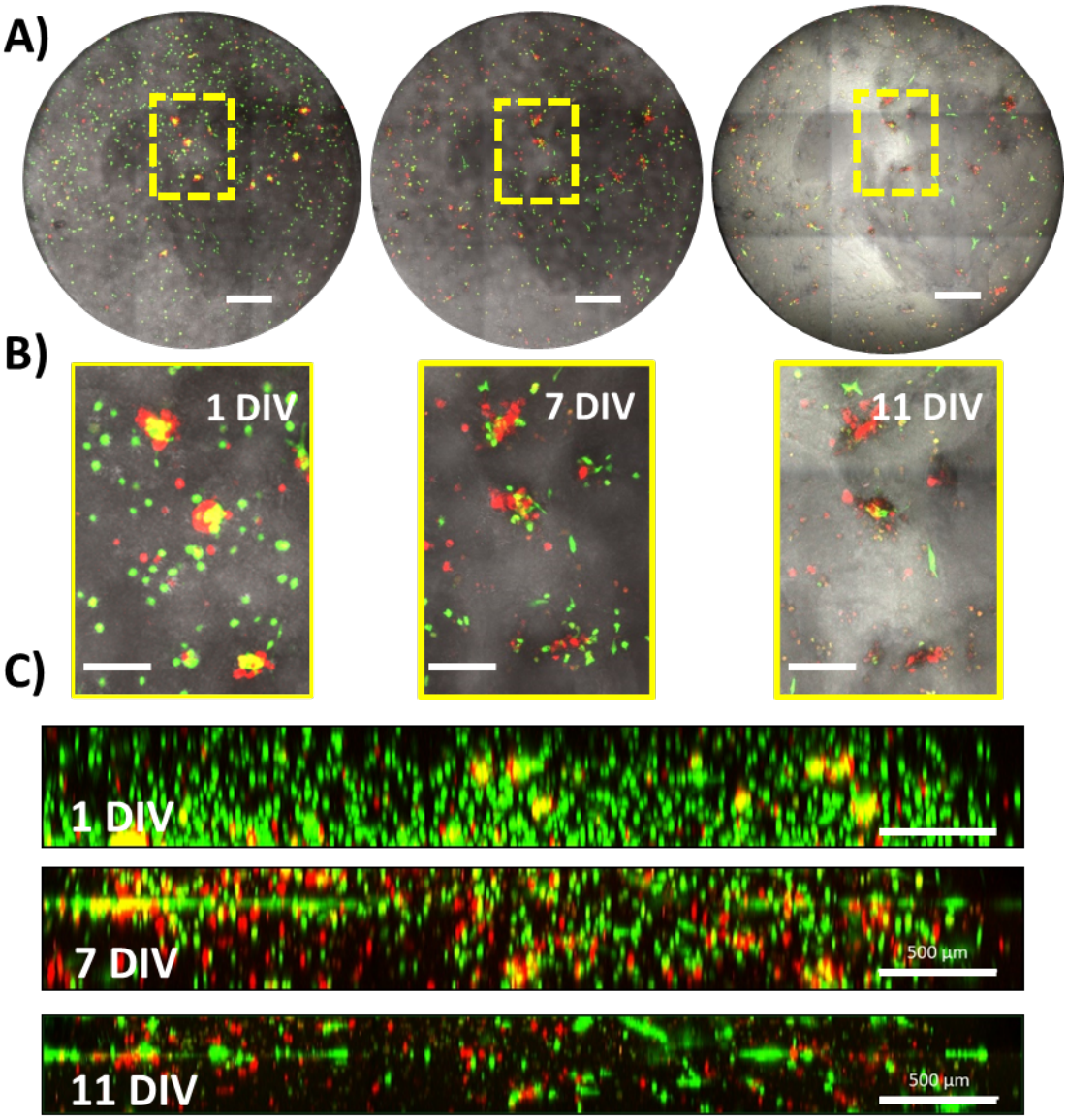

Figure S17. A) Reorganization of cells in optimized ECM, with initial clustering around pre-formed spheroids of MCF7 and HDF cells. Scale bars: 500 µm. **B)** Zoom views of the yellow dashed squares in A). Scale bars: 200 µm. **C)** XZ profiles showing cell distribution changes in control samples (no scaffold). Scale bars: 500 µm.

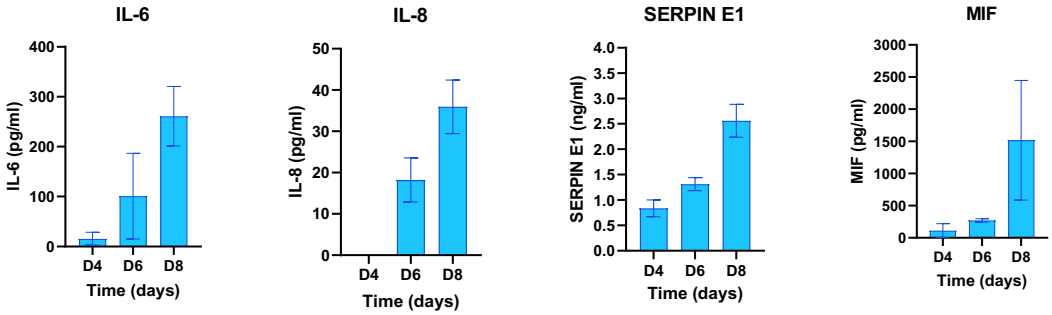

Figure S18. Cytokine production in cell/spheroid models embedded in optimized ECM in scaffolds. Supernatant samples were collected at 4, 6, and 8 DIV and frozen until analysis using DuoSet Cytokine Sandwich ELISAs. Results are the mean of triplicate samples measured in duplicate; error bars represent ±SD.

7. SERS Imaging within the scaffold + optimized ECM model

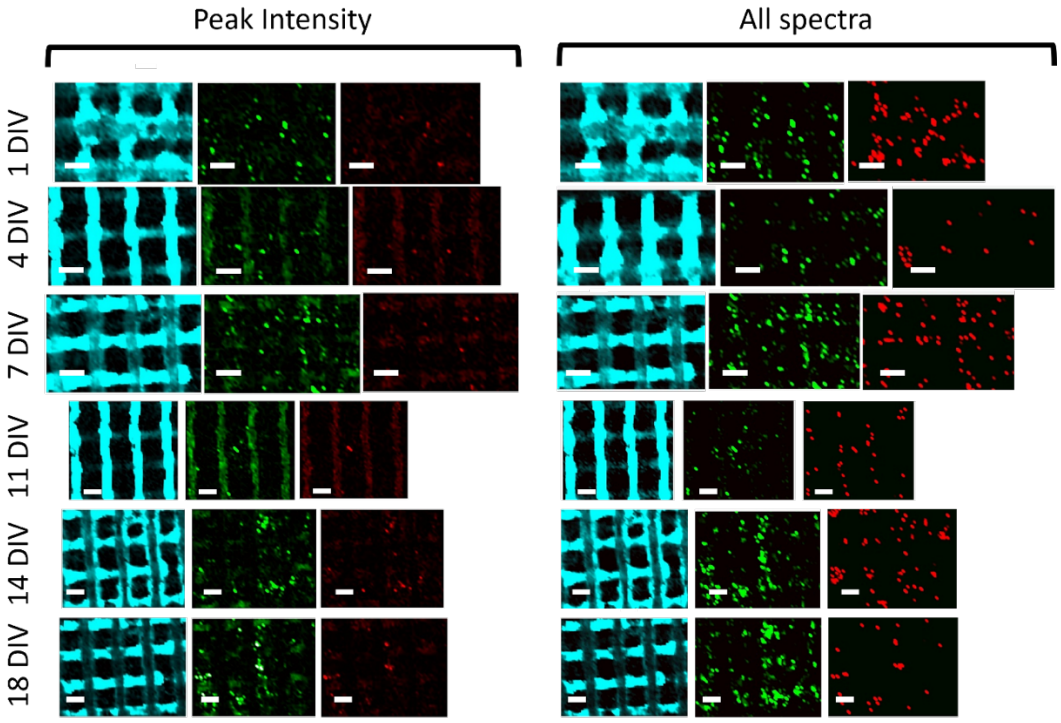

Figure S19. SERS maps of the top layer of the scaffold recording the SERS intensities of the different components of a scaffold labeled with AuNR@2NAT (cyan) containing preformed spheroids of MCF7@AuNS@BT (red) and HDF@AuNS@4BPT (green). Two different data analyses were employed to create XY maps. Left hand side images are obtained taking as a reference the peak intensity of each tag (2NAT 1380 cm^{-1}; 4BPT 1280 cm^{-1}; BT 1000 cm^{-1}), whereas right hand side images are obtained using reference spectra for each tag. Scale bars: 500 µm.

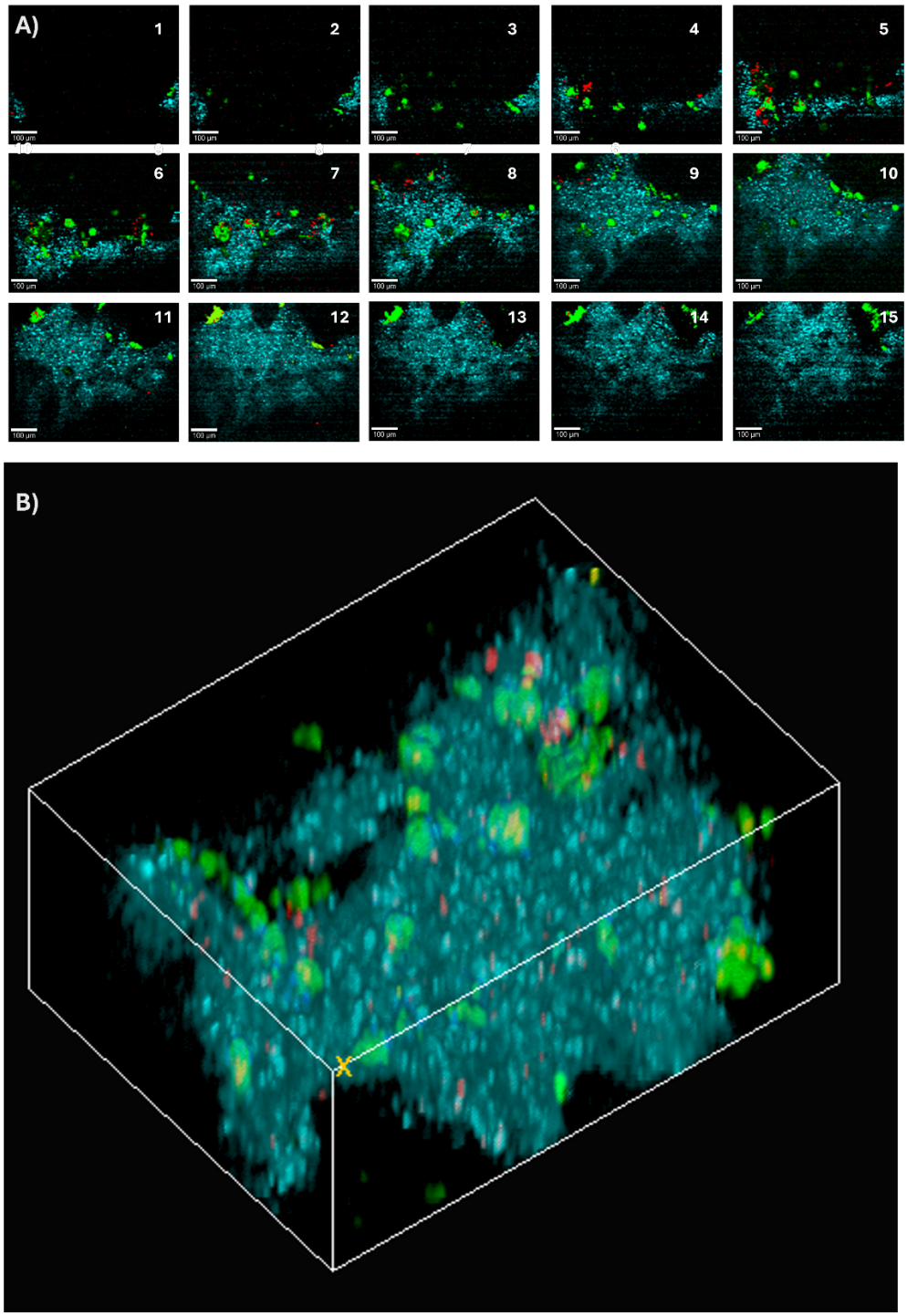

Figure S20. A) SERS maps of the different components of a scaffold labeled with AuNR@2NAT containing preformed spheroids of MCF7 cells labeled with AuNS@BT and HDF cells labeled with AuNS@4BPT. Maps were taken each 15 µm in a fixed sample after 4 DIV (Alpha300R microscope). Scale bars: 100 mm. B) 3D SERS reconstruction of the area imaged in (A) (650 µm × 500 µm × 300 µm).

8. SERS sensing

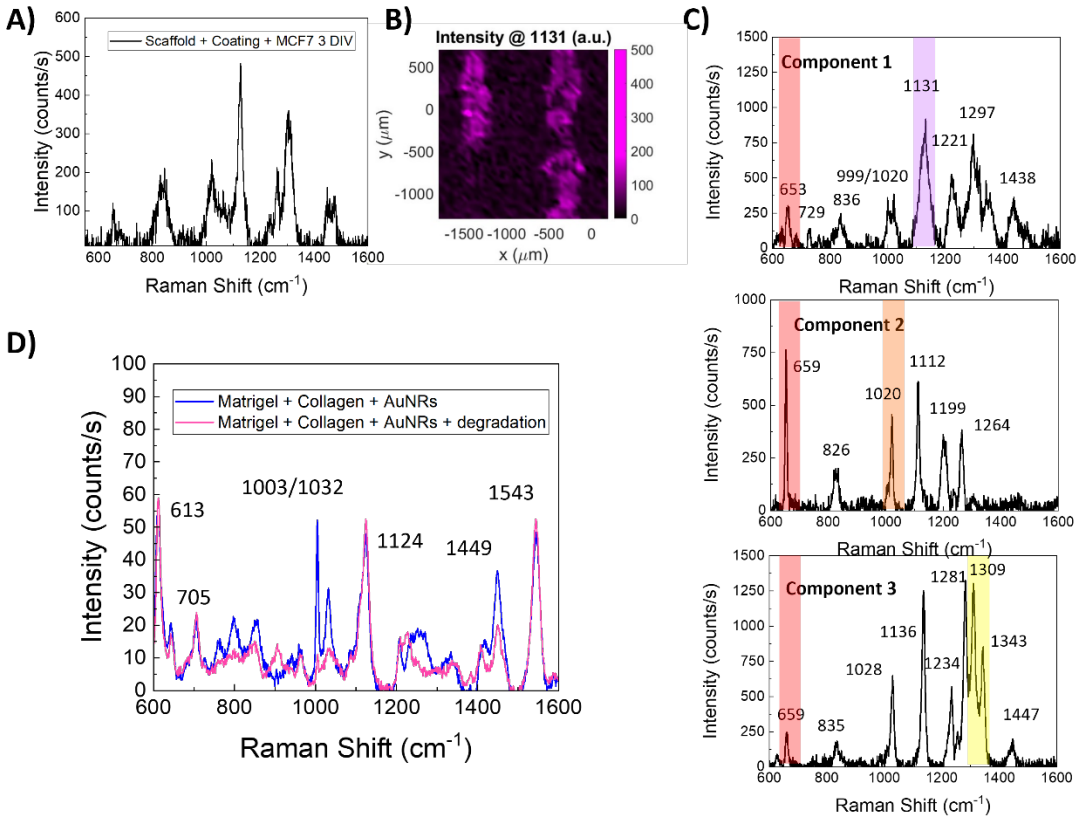

Figure S21. A) SERS spectrum of a fibronectin/collagen-coated scaffold seeded with MCF7 cells, after 3 days of incubation. **B)** SERS maps based on signal intensity at the 1131 cm^{-1} peak from the spectrum in (A). **C)** SERS spectra of the different components identified in the PCA analysis. **D)** Control SERS spectra of the 3D SERS sensing matrix before (blue) and after (pink) degradation of the ECM proteins.

9. TEM characterization of the 3D model

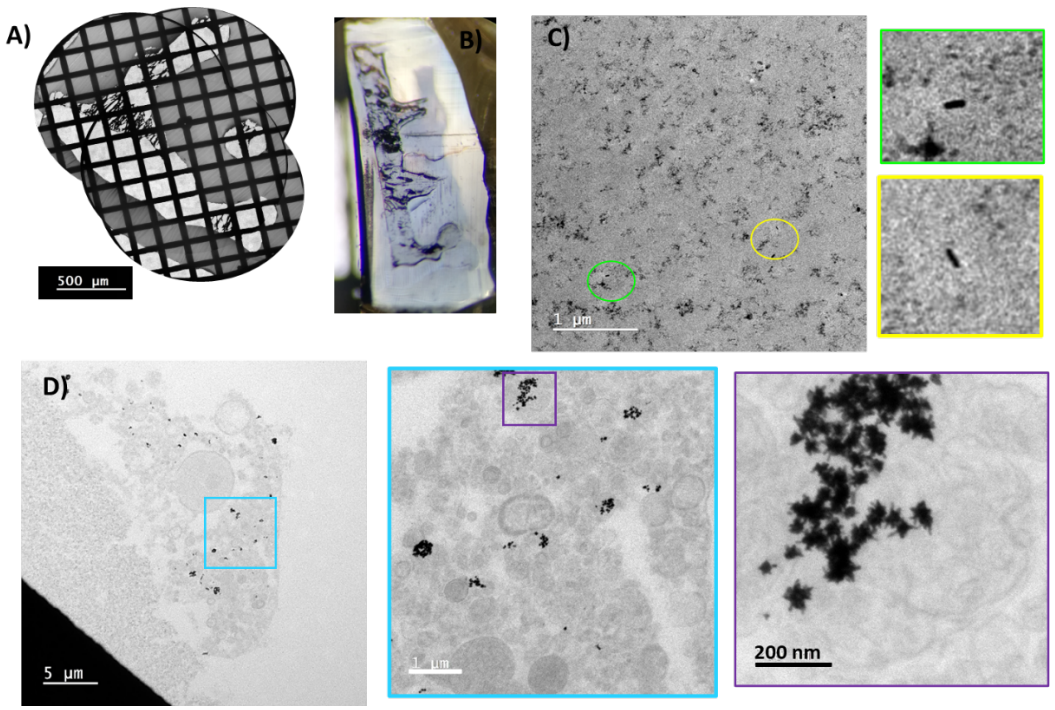

Figure S22. TEM characterization of scaffolds with cells and spheroids embedded in optimized ECM. **A)** Collage of three TEM grids supporting resin-embedded scaffold sections, observed at low-magnification. **B)** Photograph of a PEGDA scaffold embedded in resin. **C)** TEM images of the optimized ECM showing AuNRs (morphology clearly observed in zoom images from the circled areas); **D)** TEM images of a cell embedded in the optimized ECM, showing the presence of AuNSs (SERS imaging tags) but not AuNRs. Images at gradually higher magnification are also shown (blue and purple squares).

10. Temperature sensing

For local temperature measurements, we explored the incorporation of our recently developed LaOCl:Nd^{3+} nanothermometers within the hydrogel fibers.[2] These nanothermometers (average particle diameter of 19 nm, sensitivity Sr = 2.19 % K^{-1}) display various photoluminescence bands in the NIR region, centered at 820, 900, 1064, and 1350 nm (**Figure S23**). For temperature measurements, we chose to analyze the integrated intensity ratio between the 820 nm and 900 nm bands, corresponding to the highly sensitive interband transitions from the $^4F_{5/2}$ + $^2H_{9/2}$ and $^4F_{3/2}$ excited states to the $^4I_{9/2}$ ground state, respectively. Photoluminescence signals in this region can be collected regardless of the presence of SERS tags, such as AuNR@2NAT (**Figure S23C**), thus offering the possibility of using the nanothermometers within multimodal scaffolds. Reconstruction of the photoluminescence signal from the 3D printed scaffolds, which again shows the high definition of the printed constructs, confirmed a homogenous distribution of nanothermometers inside the fibers (**Figure S24A** and **S25**). To verify the accuracy of LaOCl:Nd^{3+} nanothermometers, we employed a temperature-controlled chamber, in which a thermocouple was also inserted as a reference. **Figure S25B** shows a comparison of the temperature values measured using the nanothermometers with the reference thermocouple temperature (a calibration curve for these measurements is shown in **Figure S23D**), which reveals a good overall agreement within a broad range, including biologically relevant temperatures (30 – 40 °C).

Temperature calculation

To measure local temperature, luminescence intensity ratio (LIR) based-nanothermometers were employed. LIR nanothermometers rely on the variation of the relative intensity between two luminescence bands or peaks with temperature. If these levels are close enough, it means that they are thermalized or thermally linked, and follow the Boltzmann distribution function:

$$LIR \propto B \cdot e^{\frac{-\Delta E}{k_B \cdot T}} \quad \text{(S1)}$$

where B is a constant that depends on the measured system (i.e., the medium in which the particles are embedded, the optical system used for the PL readout, etc.); ΔE is the energy difference between the states at which the transition occurs; T is the temperature; and k_B is

Boltzmann's constant (0.695 cm^{-1}/K). A commonly used parameter for determining the performance of these nanothermometers is the relative sensitivity (S_r), defined as the variation of the signal per unit of variation of the temperature, at 300 K.

$$S_r = \left| {}^{\Delta E}/_{k_B \cdot T^2} \right| \quad \text{(S2)}$$

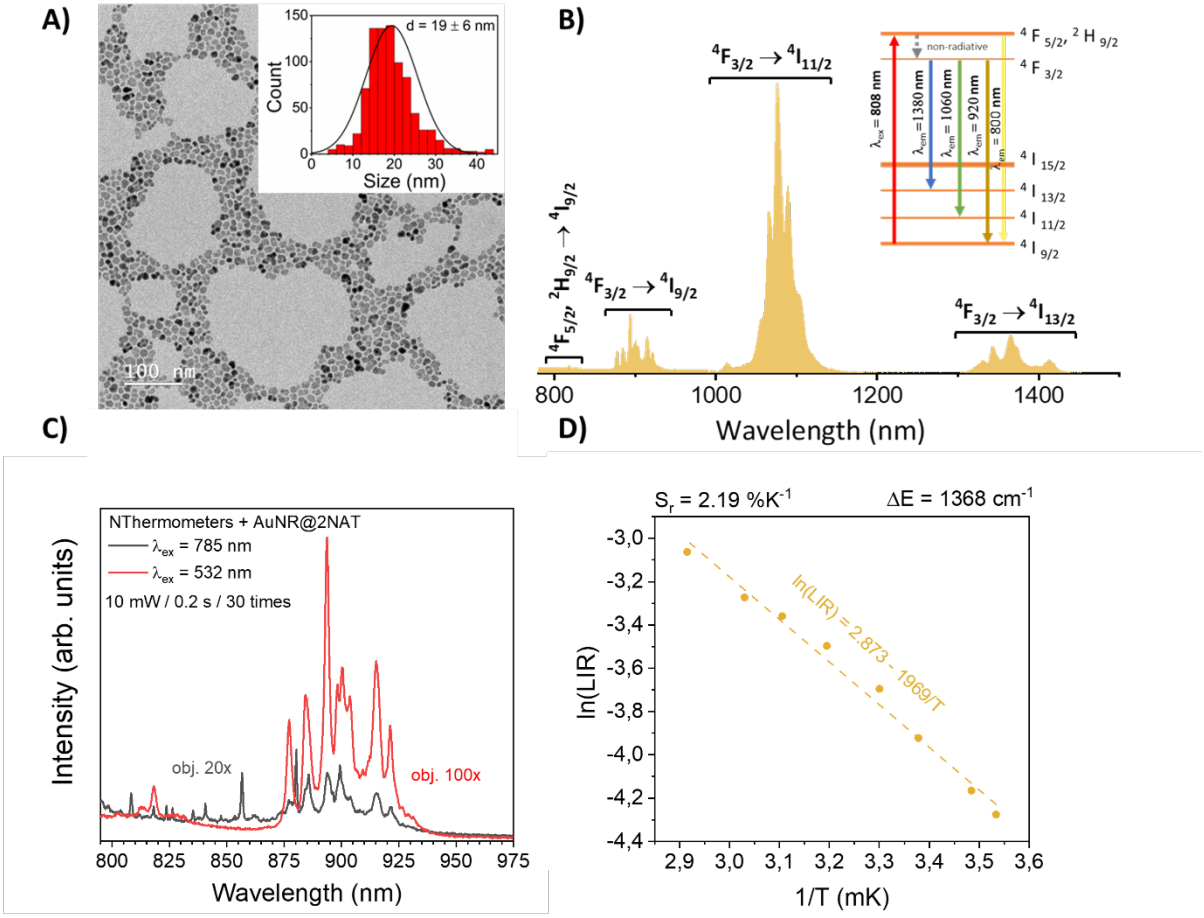

Figure S23. A) TEM image and size distribution of the nanothermometers. **B)** NIR photoluminescence spectra showing the 4 bands of Nd^{3+}-doped LaOCl. **C)** Normalized stacked SERS and NIR photoluminescence spectra, recorded to check potential interference of SERS tags with temperature measurements. **D)** Calibration curve of the nanothermometers embedded in the scaffold, with the corresponding ΔE and S_r.

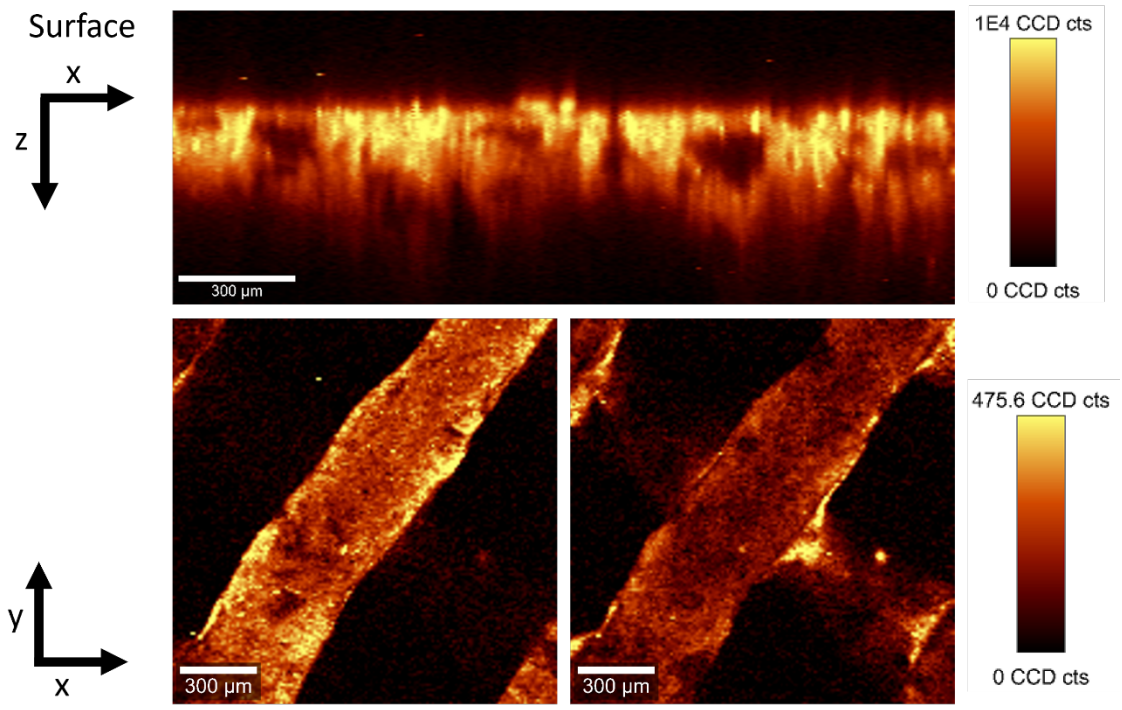

Figure S24. Nanothermometer photoluminescence imaged in XZ and XY planes, corresponding to the integral of the whole 900 nm band under a 532 nm excitation wavelength, laser power of 40 mW, and 0.01 s integration time.

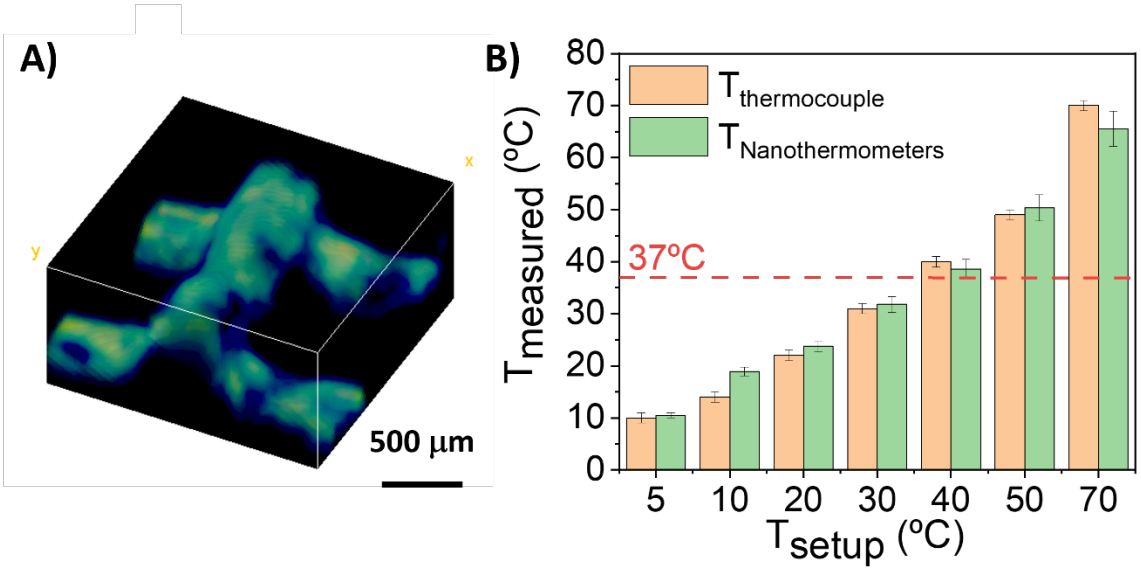

Figure S25. A) 3D reconstruction of the photoluminescence signal from LaOCl:Nd^{3+} nanothermometers embedded within the scaffold; the signal corresponds to the integral of the entire 900 nm band. B) Temperature values measured using nanothermometers (green) and compared to results from a thermocouple (orange).

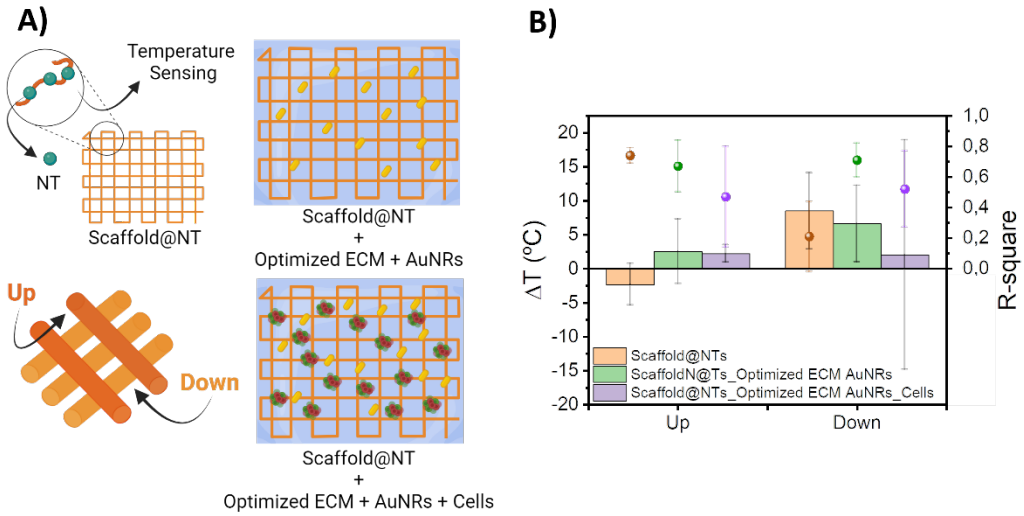

Figure S26. Temperature sensing using scaffolds containing nanothermometers (NT), with and without optimized ECM. **A)** Schematic view of the "Up" and "Down" temperature measurements in the scaffold. In the "Up" scenario, little ECM lies between the nanothermometer and the objective (top-down objective, Raman microscope setup), whereas in the "Down" scenario, considerably more ECM is present, in addition to AuNRs, cells, and/or spheroids which may distort photoluminescence signals in the optical pathway. **B)** Photoluminescence measurements conducted in "Up" and "Down" scenarios for various scaffold setups (NT-containing scaffolds alone, and with optimized ECM containing AuNRs, with and without cells/spheroids) in a chamber at 37 °C. The difference in measured temperature compared to the true chamber temperature (left axis), and the R-square from the calibrations in the different systems (right axis), are shown.

11. 3D cell model components

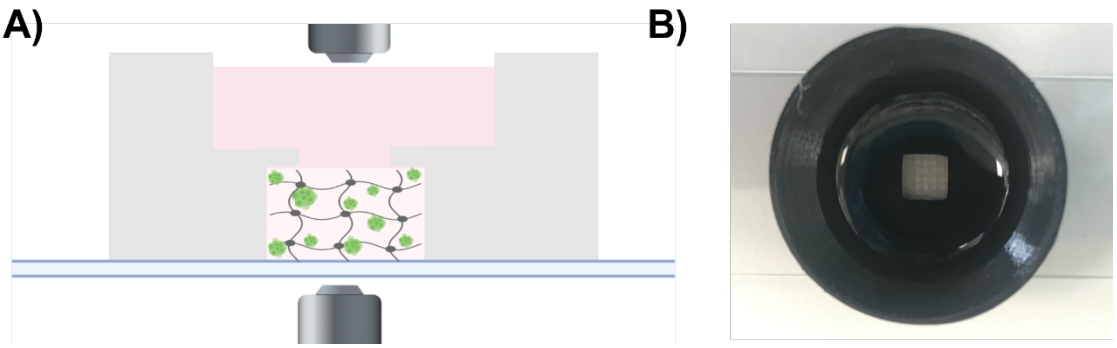

Figure S27. To measure the same sample using SERS and fluorescence imaging, a setup suitable for upright (Raman microscope) and inverted (fluorescence) microscopy was required. As such, the scaffold (with ECM and cellular components) was placed on top of a quartz glass slide or cover slip, compatible with both imaging modalities (**A**). To hold the scaffold in place on the slide, a 3D-printed PCL holder was designed, suppressing scaffold movement (in XYZ). The conical shape was designed to hold a significant amount of cell media (at least 1 mL) in addition to the insertion of immersion objectives (**B**).

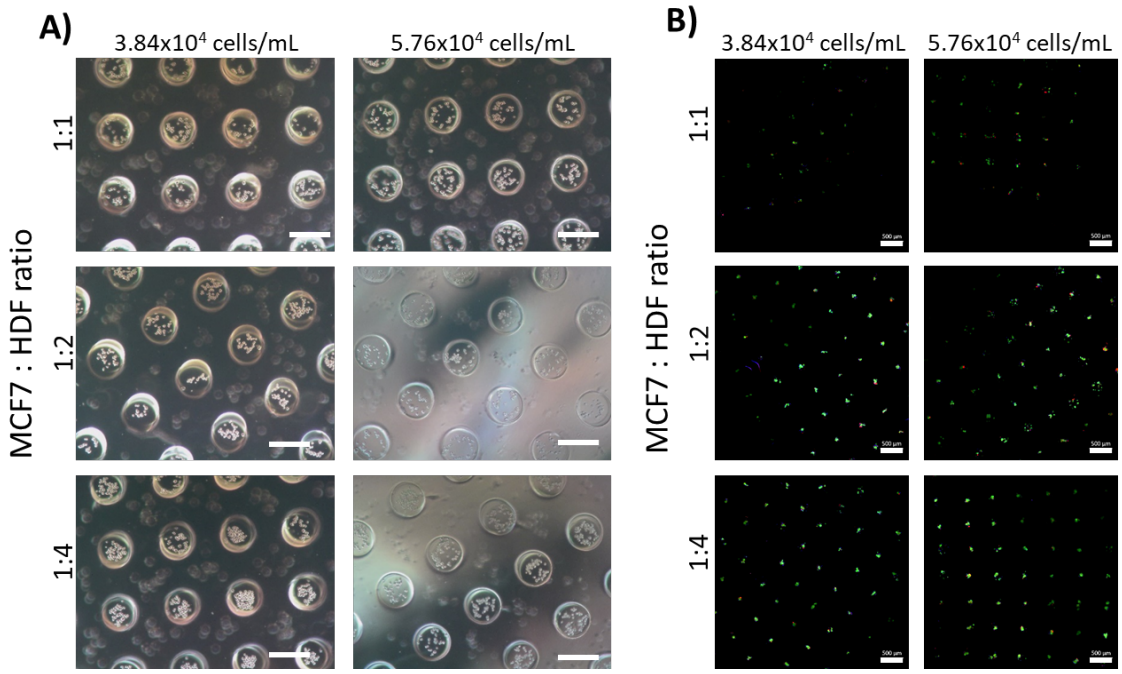

Figure S28. Spheroid formation using µ-molds. Different MCF7: HDF cell seeding ratios and numbers were tested. **A)** Phase contrast transmission light images showing microwells in which cells sediment. Images taken on the day of seeding. **B)** Confocal fluorescence microscopy images of spheroids composed of MCF (red) and HDF (green) cells. Scale bars: 500 µm.

12. Other supporting materials

Movie S1. SERS maps of the different components of a scaffold labeled with AuNR@2NAT (cyan) containing preformed spheroids of MCF7 cells labeled with AuNS@BT (red) and HDF cells labeled with AuNS@4BPT (green). SERS maps (1000 μm × 1000 μm XY) were taken after 7 DIV, at different heights of the scaffold in an imaging hole filled with optimized ECM. Scale bar in the optical image: 200 μm.

13. References

(1) Nerger, B. A.; Brun, P. T; Nelson, C. M. Microextrusion printing cell-laden networks of type I collagen with patterned fiber alignment and geometry. *Soft Matter* **2019**, *15*, 5728-5738.

(2) Renero-Lecuna, C.; Herrero, A.; Jimenez De Aberasturi, D.; Martínez-Flórez, M.; Valiente, R.; Mychinko, M.; Bals, S.; Liz-Marzán, L. M. Doped Lanthanum Oxychloride Nanocrystals as Nanothermometers. *J. Phys. Chem. C* **2021**, *125*, 19887–19896